Structure of a Single Amino Acid Mutant of Aspartate Carbamoyltransferase at 2.5-Å Resolution: Implications for the Cooperative Mechanism†

J. Eric Gouaux and William N. Lipscomb*
Gibbs Chemical Laboratory, Harvard University, Cambridge, Massachusetts 02138
Steven A. Middleton and Evan R. Kantrowitz
Department of Chemistry, Boston College, Chestnut Hill, Massachusetts 02167
Received July 28, 1988; Revised Manuscript Received October 21, 1988

ABSTRACT: One of the many interactions important for stabilizing the T state of aspartate carbamoyltransferase occurs between residues Tyr240 and Asp271 within one catalytic chain. The functional importance of this polar interaction was documented by site-directed mutagenesis in which the tyrosine was replaced by a phenylalanine [Middleton, S. A., & Kantrowitz, E. R. (1986) *Proc. Natl. Acad. Sci. U.S.A. 83*, 5866–5870]. In the Tyr240 → Phe mutant, the aspartate concentration required to achieve half-maximum velocity is reduced to 4.7 from 11.9 mM for the native enzyme. Here, we report an X-ray crystallographic study of the Tyr240 → Phe enzyme at 2.5-Å resolution. While employing crystallization conditions identical with those used to grow cytidine triphosphate ligated T-state crystals of the native enzyme, we obtain crystals of the mutant enzyme that are isomorphous to those of the native enzyme. Refinement of the mutant structure to an *R* factor of 0.219 (only eight solvent molecules included) and subsequent comparison to the native T-state structure indicate that the quaternary, tertiary, and secondary structures of the mutant are similar to those for the native T-state enzyme. However, the conformation of Phe240 in one of the two crystallographically independent catalytic chains contained in the asymmetric unit is significantly different from the conformation of Tyr240 in the native T-state enzyme and similar to the conformation of Tyr240 as determined from the R-state structure [Ke, H.-M., Lipscomb, W. N., Cho, Y. J., & Honzatko, R. B. (1988) *J. Mol. Biol.* (in press)], thereby indicating that the mutant has made a conformational change toward the R state, localized at the site of the mutation in one of the catalytic chains.

Regulation of metabolic pathways via enzymes whose activity is dependent on the concentration of various molecules is of paramount importance for all living systems. In response to a change in the concentration of some molecule, a regulatory enzyme can alter its functional properties. However, a change in function (such as the affinity for substrate) necessarily mandates a change in structure (Koshland, 1958). One excellent example of a regulatory enzyme in which there are dramatic functional and structural changes as a result of different concentrations of substrates and allosteric effectors is *Escherichia coli* aspartate carbamoyltransferase [EC 2.1.3.2; for a recent review see Kantrowitz and Lipscomb (1988)].

Comprising aspartate carbamoyltransferase are six copies each of two different types of polypeptide chains: catalytic (c, M_r 33 000) and regulatory (r, M_r 17 000; Gerhart & Schachman, 1965). In the holoenzyme, each of the two catalytic subunits consists of three c chains ($2c_3$) and each of the three regulatory subunits is made up of two r chains ($3r_2$). These subunits are arranged as shown in Figure 1 (Wiley & Lipscomb, 1968). The functions of the catalytic and regulatory subunits are, in fact, separable. The catalytic subunit catalyzes the reaction between aspartate and carbamoyl phosphate to yield the products carbamoyl aspartate and phosphate, without exhibiting cooperative behavior (Gerhart & Schachman, 1965). The regulatory subunit, r_2, binds allosteric effectors but is catalytically inactive (Gerhart & Schachman, 1965). In the holoenzyme (c_6r_6), substrates induce homotropic cooperativity, while the product of the pyrimidine pathway, cytidine triphosphate (CTP),[1] and the product of the purine pathway, adenosine triphosphate (ATP), heterotropically inhibit and activate the enzyme, respectively (Gerhart & Pardee, 1962; Bethell et al., 1968). Functionally, the homotropic cooperative properties of aspartate carbamoyltransferase are in accord with the two-state model of Monod, Wyman, and Changeux (Monod et al., 1965); the binding of substrates or suitable substrate analogues to the less active T state induces an allosteric transition to the more active R state (Foote & Schachman, 1985).

In the allosteric transition, the two catalytic trimers (c_3) separate by 12 Å along the threefold axis and rotate relative to each other by 5° around this same axis (total reorientation, 10°) while the three regulatory dimers (r_2) rotate by 15° about each of the three twofold axes of the dodecamer (Krause et al., 1987). The functional consequence of this structural reorganization is to increase the enzyme's affinity for aspartate. Although most of the structural rearrangements can be described by rigid body rotations and translations of the four domains, the loop composed of residues 230–250 in the aspartate domain (240s loop) undergoes a dramatic conformational change in the T to R transition that cannot be modeled as a rigid body movement of domains. This reorientation of

† Supported by National Institutes of Health Grant GM06920.

[1] Abbreviations: ATCase, aspartate transcarbamoylase, also called aspartate carbamoyltransferase; CTP, cytidine triphosphate; PALA, *N*-phosphonoacetyl-L-aspartate; CTP ATCase, CTP-ligated native T-state ATCase; Tyr240 → Phe ATCase, Tyr 240 → Phe T-state mutant of ATCase; PHMB, *p*-(hydroxymercuri)benzoate; $[S]_{0.5}$, substrate concentration at half the maximum observed specific activity; T and R states, less active and more active states of the enzyme usually having low and high affinity, respectively, for the substrate. To identify the same residues in the catalytic and regulatory chains related by the molecular twofold axis, a suffix of either A, B, C, or D will be appended to the residue number to indicate if the residue occupies a position in the c_1, r_1, c_6, or r_6 polypeptide chain, respectively, as shown in Figure 1.

0006-2960/89/0428-1798$01.50/0

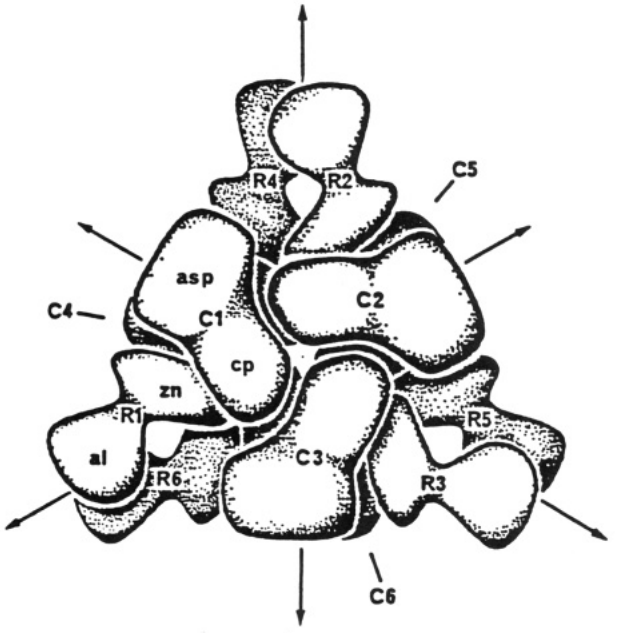

FIGURE 1: Arrangement of domains, polypeptide chains, and subunits with respect to the symmetry axes. The catalytic chains are composed of two domains, aspartate (asp) and carbamoyl phosphate (cp), and the regulatory chains also contain two domains, allosteric (al) and zinc (zn).

the 240s loop closer to the carbamoyl phosphate domain is important for the creation of an active site that has a high affinity for aspartate (Ladjimi et al., 1988), depicted in Figure 2.

The functional properties of the Tyr240 → Phe mutant have been thoroughly characterized and reflect a destabilization of the T state toward the R state. Illustrating this effect is the change in $[S]_{0.5}$ from 11.9 mM for the native enzyme to 4.7 mM for the mutant enzyme, respectively (Middleton & Kantrowitz, 1986). Moreover, because the kinetic properties for the c_3 subunit of the mutant and the native c_3 are the same, the mutation must affect only the cooperative and not the catalytic properties of the holoenzyme. In fact, because the heterotropic properties of the Tyr240 → Phe enzyme are similar to those of the native enzyme, we can more specifically assert that the mutation primarily affects the homotropic cooperativity.

Materials and Methods

Crystal Growth. The Tyr240 → Phe mutant of aspartate carbamoyltransferase, prepared and purified as previously described (Middleton & Kantrowitz, 1986), was stored at −20 °C as a 25 mg/mL solution in 1:1 (v/v) glycerol/storage buffer [40 mM K_2PO_4, 2.0 mM β-mercaptoethanol, 0.2 mM EDTA (pH 7.0)] and was dialyzed for 24 h against storage buffer prior to crystallization. The enzyme solution was diluted to 20 mg/mL with storage buffer and filtered through a 0.22-μm filter (Millipore GV). Crystallization was effected by dialyzing the enzyme solution, at room temperature, against a buffer of 40 mM sodium citrate, 1.0 mM β-mercaptoethanol, 0.2 mM EDTA, and 1.0 mM CTP with the pH adjusted to 5.8 by HCl. Typically, hexagonal plates in the space group *P*321 ($a = b = 122.2$ Å and $c = 142.5$ Å) grew in 2–3 weeks. The crystals of the Tyr240 → Phe ATCase mutant were isomorphous to crystals of the native enzyme grown under the same conditions; they diffracted to 2.4 Å. Contained in the asymmetric were two cr units related by an approximate molecular twofold axis. In preparation for data collection, crystals of dimension 0.3 × 1.0 × 1.0 mm were mounted in silanized glass capillaries that were subsequently sealed with mother liquor and melted wax.

Data Collection, Scaling, and Reduction. All of the data used for this structure determination were collected at the Biotechnology Resource, University of Virginia, on the multiwire area X-ray diffractometer (Sobottka et al., 1984). Measuring the diffracted X-rays were either two or three multiwire area detectors; a Rigaku RU-200 instrument, operating at 45 kV and 200 mA and equipped with a graphite monochromator, generated the Cu Kα radiation. The goniometer was mounted on a Huber goniostat driven by a HP-1000 computer.

Before data collection was begun, the crystal to detector distance was chosen to simultaneously maximize the density of reflections measured on each detector and minimize the number of overlapping reflections. In general the distance was 110.0 cm. Helium boxes were placed between the crystal and detector to help minimize signal attenuation due to scattering from air. Immediately following the automatic determination of the crystal orientation and refinement of detector and crystal parameters, data measurement commenced. The asymmetric unit of reciprocal space was repeatedly measured by fixing ϕ and χ and sweeping ω through values from −35.0° to +35.0° in steps of 0.07°. The average exposure time for each step was 30 s.

In this fashion, 177 399 observations were measured from three crystals with an exposure time of between 30 and 40 h for each crystal. The intensities were integrated and then corrected for background and for Lorentz and polarization factors. Using the method of Fox and Holmes (1968), the 177 399 observations of 38 679 unique reflections were scaled

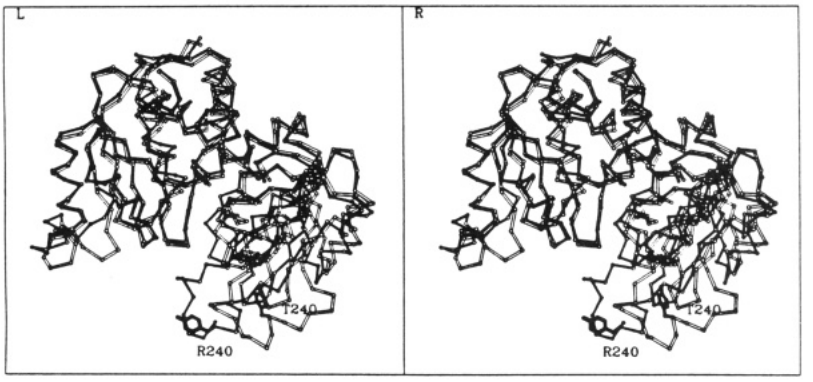

FIGURE 2: One catalytic chain of the T (unfilled lines) and R (filled lines) states. The carbamoyl phosphate domains of each chain have been superimposed on each other. Residue Tyr240 is drawn in thick filled lines in both states and labeled R240 for the R state and T240 for the T state, respectively. To help quantify the rearrangement of the 240s loop toward the carbamoyl phosphate domain, the distance that the C_α of Tyr240 moves is 8.2 Å, on the basis of this superposition. The threefold axis lies vertically in the plane of the paper.

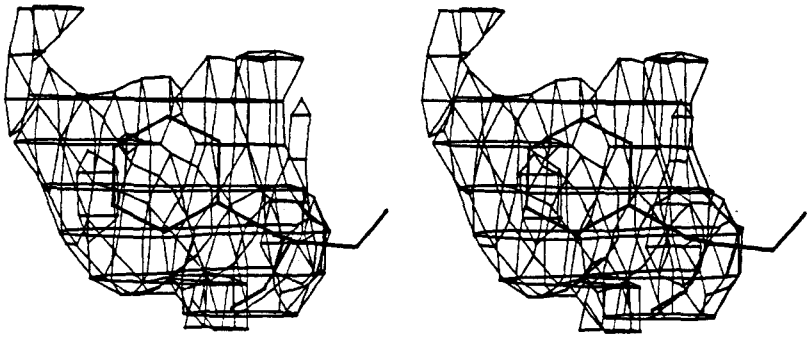

FIGURE 3: Stereo view of a portion of an omit map, calculated as described under Materials and Methods and contoured at 2σ, around residue Phe240A. The refined position of Phe240A is drawn in thick lines. Although the map is more noisy in this region of the molecule when compared to sections of the carbamoyl phosphate domain, there is sufficient density to orient the side chain. In addition, if the residue is placed in the native T-state conformation, it fits the density very poorly. Consequently, Phe240A adopts a completely different conformation from that of Tyr240A of T-state CTP ATCase. The view is similar to that in Figure 2.

together, incorrect measurements were deleted, and the data were reduced. The final R_{merge} [$R_{merge} = (\sum_{hkl}|I - \bar{I}|)/\sum_{hkl}I$] was 8.2% based on intensities, and 85.1% of the reflections had an intensity greater than $3\sigma(I)$.

Model Building and Refinement. The thoroughly refined model of the native T-state enzyme complexed with CTP (Kim et al., 1987) was used as the starting point for the refinement of the Tyr240 → Phe mutant after all of the 945 solvent molecules, the 25 residues in alternative conformations, and the 2 CTP molecules had been deleted. In addition, since the temperature factors for some of the atoms in the initial model were 2.0 (the value assigned to atoms whose temperature factor refined to a value less that 0.0), the temperature factors for all of the main-chain atoms were reset to 25.0 and those for the side-chain atoms were reset to 35.0. The computer program XPLOR (Brunger et al., 1987), installed on a CRAY-XMP/48 at the Pittsburgh Supercomputer Center, was used to refine the Tyr240 → Phe structure. The initial R factor ($R = (\sum_{hkl}||F_o| - |F_c||)/F_o$] was 0.271, using 30981 reflections from 5.0- to 2.5-Å resolution with an I/σ greater than 2.0. After 50 cycles of positional refinement, the R factor dropped to 0.25 and the rms deviations from ideality for the bond lengths and bond angles were 0.024 Å and 4.45°, respectively. Next the individual atomic temperature factors were refined, with restraints, which resulted in a further lowering of the R factor to 0.227. At this stage, an omit map was calculated by deleting residue 240 from both catalytic chains for the structure factor and phase calculation and by using $F_o - F_{c,omit240}$ for coefficients and $e^{2\pi i\alpha_{omit240}}$ for phases. On the basis of this density, it was clear that the conformation of Phe240A was different from that of the wild-type Tyr240A and that Phe240C occupied a position very similar to that of Tyr240C. Maps calculated by using coefficients $2F_o - F_c$ and phases from the Tyr240 → Phe refined structure showed excellent density for residues in the active site, where the protein was well ordered, and poorer but interpretable density in the 240s loop, where the protein was more disordered. Model building and addition of eight solvent molecules—assumed to be water molecules—near the side chain of Asp271A and Asp271C were carried out by using the graphics program FRODO (Jones, 1982), running on a Evans and Sutherland PS300 interfaced to a VAX 11/780. Subsequently, another 25 cycles of positional refinement were performed, followed by 20 cycles of restrained refinement of the temperature factors, using 33292 reflections between 6.0 and 2.4 Å that had I/σ greater than 2.0. Shown in Figures 3 and 4 are sections of a residue 240 omit map, calculated as described above. The resulting R factor was 0.219, and the rms deviations from ideality for the bond lengths and bonds angles were 0.021 Å and 4.01°, respectively. The σ of the B factors for the 1–2 atom pairs was 1.2 (target of 1.5) and the σ for the 1–3 atom pairs was 1.6 (target of 2.0). The R factor for the mutant structure of 0.219 compared well with the R factor of 0.223 for the CTP-ligated native enzyme, where the native model included no solvent molecules and was refined in a similar fashion against an analogous number of reflections between 6.0 and 2.4 Å. Although the model could be refined more exhaustively, especially by including more solvent molecules, the most significant structural information can be extracted at this level of refinement.

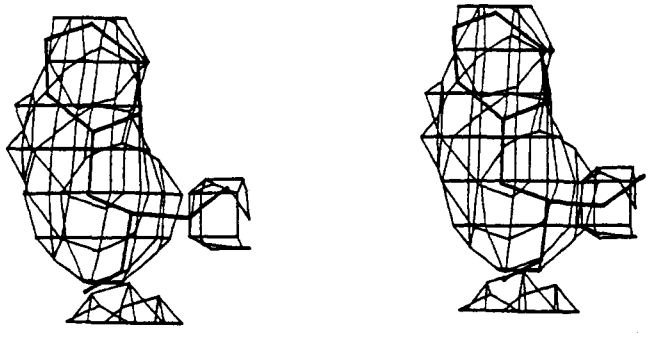

FIGURE 4: Stereo view of an omit map, analogous to that shown in Figure 3, contoured at the same level, of residue Phe240C. The density for this residue is more well-defined than for residue 240A.

RESULTS

Conformation of Residue 240 in the Catalytic Chain of the Tyr240 → Phe Mutant. The most dramatic difference between the native T state and the Tyr240 → Phe structures is the conformation of residue 240 in the catalytic chain. In the A (c_1) chain of the mutant, the phenylalanine residue has rotated approximately 90° around the C_α–C_β bond; the aromatic ring now lies in a pocket formed by residues 232A–237A. In contrast, the conformation of Phe240C in the C (c_6) catalytic chain is similar to the conformation of Tyr240C in the T form of the native enzyme. Figures 5 and 6 illustrate these results. There are no other large structural differences in the protein between the mutant and native enzymes; the rms differences in main-chain and side-chain positions are 0.32 and 0.55 Å, respectively. Using relationships derived by Luzzati (1952), we estimate an upper limit on the root-mean-square error in the coordinate positions for which there is good electron density to be approximately 0.45 Å. In regions of poor electron density, like the 240s loop, the uncertainty in the atomic positions is probably closer to 1.0 Å. However, the terminal atoms in the side chain of residue 240A of the Tyr240 → Phe enzyme occupy a position 4–5 Å from the

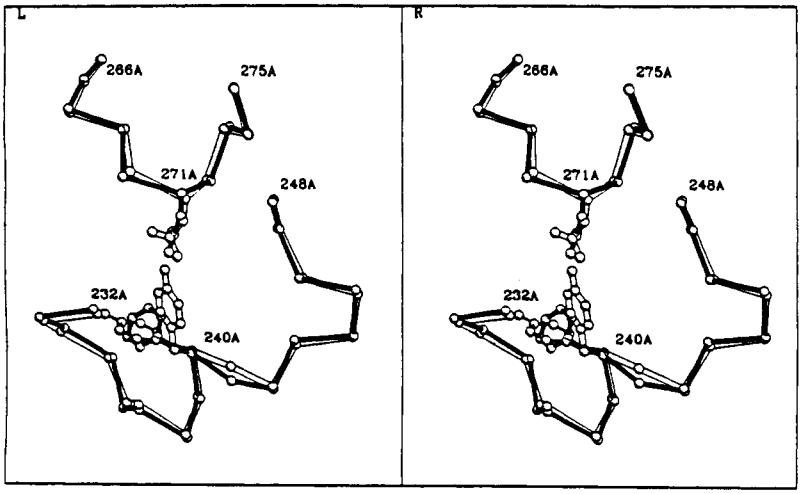

FIGURE 5: Refined positions of the 240s and 270s loops and residues 240 and 271 in the A catalytic chain. The thick filled lines correspond to the Tyr240 → Phe ATCase structure, and the unfilled lines represent the CTP ATCase model. In thin filled lines is Tyr240 in the conformation it assumes in the PALA ATCase structure. The threefold axis is in the plane of the paper and vertical. Note the similarity in the conformations of Phe240A (T state) and Tyr240A from PALA ATCase (R state).

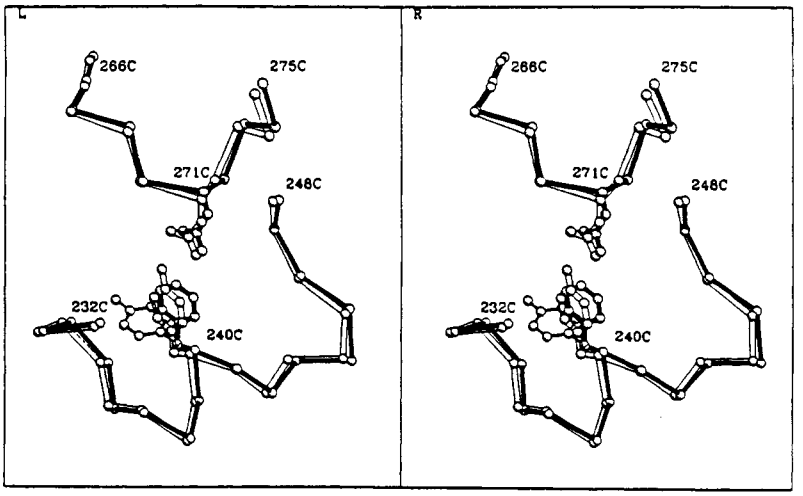

FIGURE 6: Analogous to Figure 5 and from approximately the same perspective except that these residues are from the C catalytic chain.

position of the analogous atoms in the native T-state enzyme. Consequently, the new conformation of 240A in the mutant is significant, even taking into account the uncertainty of the atomic coordinates. The refined coordinates for the Tyr240 → Phe T-state mutant of ATCase have been submitted to the Brookhaven Protein Data Bank.

Since the mutant enzyme structure belongs to the space group *P*321 and there are two molecules in the unit cell, we know that the asymmetric unit is composed of two catalytic and regulatory pairs or two cr units, each c chain comprising one-third of each of the two catalytic trimers, and the two r chains making up a regulatory dimer, linking the upper and lower catalytic trimers. Now because the crystallographic threefold axis coincides with the molecular threefold axis, the holoenzyme is generated by applying the threefold symmetry operation to the crrc entity in the asymmetric unit. The second molecule in the unit cell is then created by applying the crystallographic twofold operation. Consequently, in the mutant enzyme, the conformation of the three Phe240 residues in each of the upper and lower catalytic subunits will be the same as the conformation of Phe240 in the A and C catalytic chains in the asymmetric unit, respectively. In other words, the threefold operation generates the two catalytic subunits from the two catalytic chains.

Conformation of Residue 271 in the Catalytic Chain of the Mutant Enzyme. Results from the refinement and from omit maps (calculated in an analogous fashion as for residue 240, described under Materials and Methods) indicate that the position of Asp271 in either catalytic chain is not affected by the mutation, at this limit of resolution.

Table I: Average *B* Factors (Å^2) for CTP (Native) and Tyr240 → Phe (Mutant) ATCase

residues	native	mutant
A1–A160	15.1	25.5
A230–A250	42.2	55.0
ΔB^a	27.1	29.5
C1–C160	11.7	19.3
C230–C250	42.1	53.2
ΔB^a	30.4	33.9

[a] ΔB refers to the difference in average *B* factors between the 240s loop (residues 230–250) and the carbamoyl phosphate domain (residues 1–160) for the A (c_1) and C (c_6) catalytic chains.

Analysis of the B (Temperature) Factors for the 240s Loop, in the Catalytic Chain, in the Tyr240 → Phe Mutant. When we determine the average *B* factors for the carbamoyl phosphate domain (residues 1–160) and the 240s loop (residues 230–250) for both the CTP and Tyr240 → Phe ATCase structures, we find that in the Tyr240 → Phe structure the difference between these two regions is slightly larger than in the CTP ATCase structure as shown in Table I. The larger difference between the *B* factors for the carbamoyl phosphate

domain and the 240s loop for the Tyr240 → Phe mutant is similar in both of the crystallographically independent catalytic chains in the asymmetric unit. However, the difference between the average *B* factor for the carbamoyl phosphate domain and the average *B* factor for residue 240 in Tyr240 → Phe ATCase is actually slightly smaller than the difference between the analogous quantities determined from the CTP ATCase structure.

Discussion

Chemical modification (Landfear et al., 1978a,b) and site-directed mutagenesis (Middleton & Kantrowitz, 1986) studies have demonstrated the importance of tyrosine 240 in the catalytic chain for the homotropic cooperative properties of aspartate carbamoyltransferase. Nuclear magnetic resonance (Wacks & Schachman, 1985a,b) experiments have shown that the spectroscopic properties of some of the tyrosine residues differ in the T and R states, although the specific assignments for the 11 tyrosine residues in the catalytic and regulatory chains were not determined. In this study, we have focused on one particular tyrosine residue, tyrosine 240. By combining the techniques of site-directed mutagenesis with X-ray crystallography, we have probed the relationship between structure and function in aspartate carbamoyltransferase in a very selective and controlled fashion.

The most straightforward structural explanation for the difference in function between the native and mutant enzymes is grounded in the native CTP-ligated T-state structure (Kim et al., 1987). Here, the hydroxyl group of Tyr240 may form a hydrogen bond to the carboxylate of Asp271, stabilizing the T state. In the PALA-ligated R-state ATCase structure (Krause et al., 1987), the hydroxyl of Tyr240 is not in a position to hydrogen bond to any other residue. Consequently, removal of the hydroxyl group by the mutation Tyr240 → Phe should preferentially destabilize the T state, without affecting the stability of the R state. This explanation is substantiated by the results from the kinetics experiments (Middleton & Kantrowitz, 1986; Hsuanyu et al., personal communication).

However, in the crystal structure of Tyr240 → Phe ATCase, we see only a small perturbation from the structure of CTP ATCase. Furthermore, the difference in structure is localized to only one of the catalytic chains in the asymmetric unit of the crystal, the A chain. One explanation for the asymmetry of Phe240 is that the packing of molecules in the crystal might differentially perturb one of the catalytic chains and render the environment around Phe240A different from that of Phe240C. In fact, for CTP ATCase, the interaction between Tyr240 and Asp271 is different in the two catalytic chains in the crystallographic asymmetric unit. The distance between the hydroxyl group of Tyr240A and the closest side-chain oxygen of Asp271A is 3.5 Å, close enough for a weak hydrogen bond. However, the hydroxyl group of Tyr240C is 4.2 Å from the closest oxygen atom of residue Asp271C—too far to form a hydrogen bond. If this asymmetry in the A and C catalytic chains is also common to the mutant, it could explain why Phe240A has rotated away from the side chain of Asp271A and why Phe240C has not; Phe240A, closer to the carboxylate of Asp271A than Phe240C is to the carboxylate of Asp271C, might rotate about the C_α–C_β bond to avoid the interaction between the phenylalanine ring and the negative charge on Asp271A's side chain. Phe240A might also reorient to allow solvent to hydrate the charge on Asp271A's carboxylate. Intermolecular interactions for the A chain are significantly greater than for the C chain in both the CTP-ligated T structure and the Tyr240 → Phe structure. These interactions occur near the c_1r_1 interface and may play some role in the different conformations of Phe240A and Phe240C.

One consequence of the T to R transition in the native enzyme is that the c_α of residue 240 relocates 8.2 Å closer to the carbamoyl phosphate domain and the average χ_1 dihedral angle changes from −169° (T) to −78° (R). The χ_1 dihedral angles for the mutant and native proteins assume values commonly seen elsewhere (Janin & Wodak, 1978). Indeed, the χ_1 angle determined from the refinement—and not from model building—for residue Phe240A of the Tyr240 → Phe ATCase closely matches the χ_1 angle of Tyr240A in the PALA ATCase structure. On the basis of the crystal structure, the mutation changes the local conformation of Tyr240 → Phe ATCase to an R-like structure without triggering the quaternary structural transition. The T quaternary structure of the mutant enzyme has been confirmed in solution by low-angle X-ray scattering experiments. Thus, the mutant enzyme, in the absence of substrates or substrate analogues, exists predominantly in the T state (P. Vachette, personal communication).

One unusual property of Tyr240 → Phe ATCase is its 7-fold increase in reactivity with *p*-(hydroxymercuri)benzoate (PHMB) in the absence of active-site ligands when compared to the native enzyme (Middleton & Kantrowitz, 1986). Historically, a change in the enzyme's reactivity with mercurials would be interpreted as indicative of a change in the conformation of the enzyme (Gerhart & Schachman, 1968; Blackburn & Schachman, 1977; Middleton & Kantrowitz, 1986). The validity of this method for establishing the quaternary conformational state is severely questioned. The structure of Tyr240 → Phe ATCase as determined from this study is very similar to that of CTP ATCase, even though the PHMB reactivity is dramatically different from that of the native T-state enzyme and much more like the reactivity of the R state.

Often information concerning the flexibility of proteins can be extracted from the refined atomic temperature factors or *B* factors (Ringe & Petsko, 1985). Unfortunately, the comparison of the absolute values of the *B* factors determined from moderate resolution data (ca. 2.5 Å) is probably not meaningful (Ringe & Petsko, 1985). Consequently, we compare the relative difference in the temperature factors between a well-ordered region of the enzyme and the 240s loop in CTP and Tyr240 → Phe ATCase. The relative differences in the average *B* factors between the carbamoyl phosphate domains (residues 1–160) and the 240s loops (residues 230–250) in Tyr240 → Phe and CTP ATCase are shown in Table I. For Tyr240 → Phe ATCase, the difference between the carbamoyl phosphate domain and the 240s loop is slightly larger in both of the crystallographically independent catalytic chains, implying that in the mutant the 240s loop is more flexible than in CTP ATCase. The mutation seems to increase the disorder of the whole 240s loop and not the disorder of the residue itself, as illustrated by the smaller difference in the average *B* factor between the residue 240 and the carbamoyl phosphate domain, in both the A and C catalytic chains, when compared to the difference in the average *B* factor between the residue 240 and the carbamoyl phosphate domain in CTP ATCase. This increased disorder in the 240s loop of the mutant might facilitate the allosteric transition. However, it is possible that intermolecular contacts in the crystal restrict the fluctuations and conformational substates of the 240s loop, and the mobility of this region of the mutant might be even greater in solution.

In conclusion, we find that the CTP-ligated structure of the Tyr240 → Phe mutant of aspartate carbamoyltransferase is very similar to the structure of the CTP-ligated native enzyme.

The local conformation of residue 240 in the A chain is similar to its conformation in the PALA complex (Krause et al., 1987), indicating that one conformational change involved in the T to R transition has taken place without triggering the quaternary conformational change. Indeed, these results imply that the mechanism for the allosteric transition at the level of individual residues might follow a stepwise as compared to a concerted mechanism.

ACKNOWLEDGMENTS

We thank Professors R. Kretsinger and S. Sobottka of the University of Virginia for use of an area detector for collection of the X-ray diffraction data on this derivative and R. Chandros, B. Justice, and T. Ptak for help with data collection and processing. We also acknowledge Professor N. Xuong of the University of California at San Diego for use of an area detector for earlier data collection on PALA ATCase. We are grateful to Axel Brunger for help in setting up XPLOR. We also thank the Pittsburgh Supercomputing Center for computer use.

Registry No. ATCase, 9012-49-1; L-Tyr, 60-18-4; L-Phe, 63-91-2.

REFERENCES

Baillon, J., Tauc, P., & Hervé, G. (1985) *Biochemistry 24*, 7182–7187.

Bethell, M. R., Smith, K. E., White, J. S., & Jones, M. E. (1968) *Proc. Natl. Acad. Sci. U.S.A. 60*, 1442–1449.

Blackburn, M. N., & Schachman, H. K. (1977) *Biochemistry 16*, 5084–5091.

Brunger, A. T., Kuriyan, J., & Karplus, M. (1987) *Science 235*, 458–460.

Foote, J., & Schachman, H. K. (1985) *J. Mol. Biol. 186*, 175–184.

Foote, J., Lauritzen, A. M., & Lipscomb, W. N. (1985) *J. Biol. Chem. 260*, 9624–9629.

Fox, G. C., & Holmes, K. C. (1966) *Acta Crystallogr. 20*, 886–891.

Gerhart, J. C., & Pardee, A. B. (1962) *J. Biol. Chem. 237*, 891–896.

Gerhart, J. C., & Schachman, H. K. (1965) *Biochemistry 4*, 1054–1062.

Gerhart, J. C., & Schachman, H. K. (1968) *Biochemistry 7*, 538–552.

Janin, J., Wodak, S., Levitt, M., & Maigret, B. (1978) *J. Mol. Biol. 125*, 357–386.

Jones, T. A. (1982) in *Computational Crystallography* (Sayre, D., Ed.) pp 303–317, Oxford, London.

Kantrowitz, E. R., & Lipscomb, W. N. (1988) *Science 241*, 669–674.

Ke, H.-M., Lipscomb, W. N., Cho, Y. J., & Honzatko, R. B. (1988) *J. Mol. Biol.* (in press).

Kim, K. H., Pan, Z., Honzatko, R. B., Ke, H.-M. & Lipscomb, W. N. (1987) *J. Mol. Biol. 196*, 853–875.

Koshland, D. E., Jr. (1958) *Proc. Natl. Acad. Sci. U.S.A. 44*, 98–104.

Krause, K. L., Volz, K. W., & Lipscomb, W. N. (1987) *J. Mol. Biol. 193*, 527–553.

Ladjimi, M. M., & Kantrowitz, E. R. (1988) *Biochemistry 27*, 276–283.

Ladjimi, M. M., Middleton, S. A., Kelleher, K. S., & Kantrowitz, E. R. (1988) *Biochemistry 27*, 268–276.

Landfear, S. M., Lipscomb, W. N., & Evans, D. R. (1978a) *J. Biol. Chem. 253*, 3988–3996.

Landfear, S. M., Evans, D. R., & Lipscomb, W. N. (1978b) *Proc. Natl. Acad. Sci. U.S.A. 75*, 2654–2658.

Luzzati, V. (1952) *Acta. Crystallogr. 5*, 802–810.

Middleton, S. A., & Kantrowitz, E. R. (1986) *Proc. Natl. Acad. Sci. U.S.A. 83*, 5866–5870.

Monod, J., Wyman, J., & Changeux, J.-P. (1965) *J. Mol. Biol. 12*, 88–118.

Ringe, D., & Petsko, G. A. (1985) *Prog. Biophys. Mol. Biol. 45*, 197–235.

Sobottka, S. E., Cornick, G. G., Kretsinger, R. H., Rains, R. G., Stephens, W. A., & Weissman, L. J. (1984) *Nucl. Instrum. Methods 220*, 575–581.

Wacks, D. B., & Schachman, H. K. (1985a) *J. Biol. Chem. 260*, 11651–11658.

Wacks, D. B., & Schachman, H. K. (1985b) *J. Biol. Chem. 260*, 11659–11662.

Wiley, D. C., & Lipscomb, W. N. (1968) *Nature (London) 218*, 1119–1121.